Electronic Supplementary Information

Antiferromagnetic Proximity Coupling between Semiconductor Quantum Emitters in WSe_2 and van der Waals Ferromagnets

Na Liu[1,2], Cosmo M. Gallaro[1,2], Kamran Shayan[3,4], Arunabh Mukherjee[3,4], Bumho Kim[5], James Hone[5], Nick Vamivakas[3,4,6], Stefan Strauf[1,2]*

[1]Department of Physics, Stevens Institute of Technology, Hoboken, New Jersey 07030, United States.

[2]Center for Quantum Science and Engineering, Stevens Institute of Technology, Hoboken, New Jersey 07030, United States

[3]The Institute of Optics, University of Rochester, Rochester, New York 14627, United States.

[4]Center for Coherence and Quantum Optics, University of Rochester, Rochester, New York 14627, United States.

[5]Department of Mechanical Engineering, Columbia University, New York 10027, United States.

[6]Department of Physics and Astronomy, University of Rochester, Rochester, New York 14627, United States.

*Address correspondence to: sstrauf@stevens.edu

Supplementary Note 1. Determination of layer thickness for the ferromagnetic crystals

The magnetic material properties of vdW crystals such as their Curie temperature are strongly related to their thickness, particularly when exfoliating from a few layers down to the monolayer limit[1,2]. In contrast, the CGT and FeGT crystals utilized in this study remain with values of 55-150 nm in the "bulk-limit", and thus show ferromagnetic properties (antiferromagnetic if oxidized) that are bulk-like. The AFM line scans shown in Figure S1 reveal a layer thickness for the Fe_3GT sample of 150 nm (Fig.S1c) and a thickness of around 100 nm for the Fe_5GT sample (Fig.S1d), while the CGT comparison sample has a step height of 55 nm (Fig.S1e).

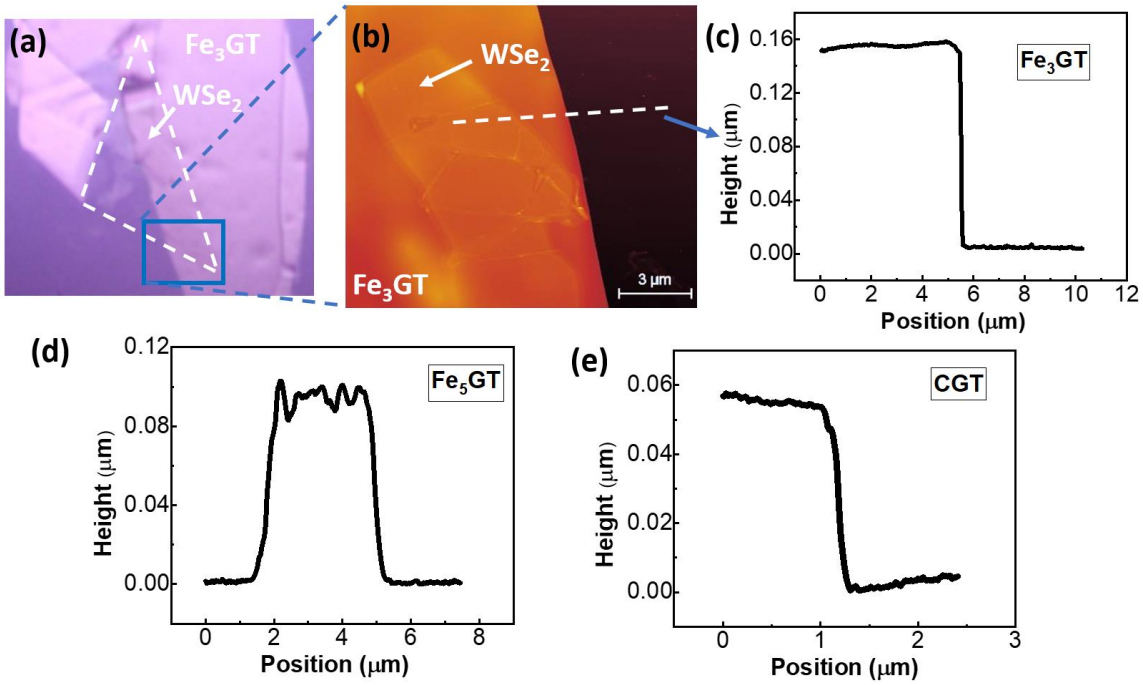

Figure S1: Atomic-force microscope (AFM) measurement of step height. (a) Optical-microscope image of an assembled Fe_3GT/WSe_2 heterostructure. (b) Corresponding AFM image recorded from the area highlighted with the blue rectangle. (c) AFM line scan across the white dotted line shown in panel (b) yields a thickness of 150 nm. Similar AFM line scans are shown for the Fe_5GT/WSe_2 heterostructure (d) and the CGT/WSe_2 heterostructure (e) with layer thickness of 100 nm and 55 nm, respectively.

Supplementary Note 2. Surface darkening effect for Fe_3GT and Fe_5GT.

Air oxidization is a common effect in 2D material such as black phosphorus and was recently also reported for Fe_3GT to lead to a thin surface oxide with a thickness of 1-2 nm if exposed for 7 min[2]. For prolonged exposure of several weeks these oxide layers can grow to tens of nm thickness[3]. In our fabrication process the typical air exposure duration is about 30-60 min before forming the heterostructures with WSe_2, leading to an omnipresent thin oxide layer on top of the Fe_3GT and Fe_5GT crystals that is encapsulated by the WSe_2 monolayer. Samples utilizing Fe_3GT look initially

clear in optical microscope images with the typical faint intensity contrast when monolayer WSe_2 is transferred on top, as shown in **Fig. S2a** by the dashed triangle. After prolonged storage of 170 days one can observe a significant darkening of the heterostructure region, as highlighted by the arrow in Figure **Fig. S2b**. In contrast, the exfoliated Fe_5GT flake shown in **Fig.S2c** develops surface darkening already within a few seconds after layer transfer if the Fe_5GT crystal is thinner than 100 nm (region highlighted by the arrow). However, for thicker crystals (>100 nm) surface darkening was not observed. It is likely that this pronounced surface darkening is an image contrast that forms when the surface oxide continues to grow. Note that for the data recorded in the main manuscript we have only utilized heterostructures where surface darkening was not present.

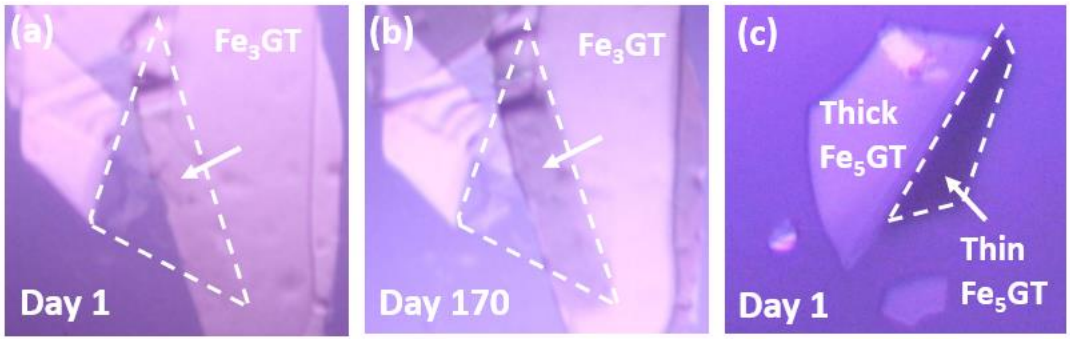

Figure S2: Observation of surface darkening in Fe_3GT and Fe_5GT. (a) Optical microscope image of Fe_3GT/WSe_2 heterostructure recorded immediately after the transfer process was completed (day 1). The heterostructure region is highlighted by the white arrow and the monolayer WSe_2 is outlined by the dashed triangle (b) Optical image of the same Fe_3GT/WSe_2 heterostructure recorded after 170 days showing significantly darkened in the heterostructure region. (c) Optical image of Fe_5GT recorded after immediately transfer the process. The region with significantly thinner Fe_5GT which darkens rapidly is enclosed by the dashed line.

	Fe_3GT emitter				**Fe_5GT emitter**		
Wavelength	723nm	732nm	749nm	772nm	722nm	752nm	760nm
Energy(eV)	1.715	1.694	1.656	1.606	1.717	1.649	1.632
G factor	9	9.5	5.8	8.5	8	6	5.5
Saturation field (T)	0.8	1.2	1	1.2	1	1.5	1.1
0T-split (meV)	0.734	0.673	0.398	0.458	0.724	0.571	0.472
Max-difference (meV)	0.08	0.09	0.12	0.1	0.07	0.066	0.086

Supplementary Table 1: Magneto-optical properties for 7 different quantum emitters residing in heterostructures with Fe_3GT and Fe_5GT. Wavelength and energy are stated for the exciton transition line with the highest intensity of the doublet. The fine-structure splitting energy is determined at zero magnetic field strength (0T-split). All emitters display antiferromagnetic coupling with ΔM values determined from the hysteresis slopes (Max-difference) as stated in the last row.

References:

[1] Gong, C.; Li, L.; Li, Z.; Ji, H.; Stern, A.; Xia, Y.; Cao, T.; Bao, W.; Wang, C.; Wang, Y.; et al. Discovery of Intrinsic Ferromagnetism in Two-Dimensional van der Waals Crystals. *Nature* **2017**, 546, 265−269.

[2] Tan, C.; Lee, J.; Jung, S.; Park, T.; Albarakati, S.; Partridge, J.; Field. M. R.; McCulloch, D. G.; Wang, L.; Lee, C. Hard Magnetic Properties in Nanoflake Van Der Waals Fe_3GeTe_2. *Nat. Commun.* **2018**, 9, 1554.

[3] Kim, D.; Park, S.; Lee, J.; Yoon, J.; Joo, S.; Kim, T.; Min, K.; Park, S.; Kim, C.; Moon, K.; Lee, C.; Hong, J.; Hwang, C. antiferromagnetic Coupling of Van der Waals Ferromagnetic Fe_3GeTe_2. *Nanotechnology*, **2019**, 30. 245701.